2022 25th International Conference on Electrical Machines and Systems (ICEMS) | 978-1-6654-9302-4/22/$31.00 ©2022 IEEE | DOI: 10.1109/ICEMS56177.2022.9982919

Direct Speed Regulation for PMSM Drive System Via a Generalized Dynamic Predictive Control Approach

1st Zhongkun Cao
College of Automation Engineering,
Shanghai University of Electric Power
Shanghai, China
zhongkuncao@163.com

2nd Jianliang Mao
College of Automation Engineering,
Shanghai University of Electric Power
Shanghai, China
jl_mao@shiep.edu.cn

3rd Xin Dong
College of Automation Engineering,
Shanghai University of Electric Power
Shanghai, China
dongxin@mail.shiep.edu.cn

4th Chuanlin Zhang
College of Automation Engineering,
Shanghai University of Electric Power
Shanghai, China
clzhang@shiep.edu.cn

***Abstract*—Aiming to improve the dynamic performance and disturbance rejection ability of the PMSM speed regulation system, this paper investigates a novel generalized dynamic predictive control (GDPC) strategy with an autonomous horizon tuning mechanism based on the non-cascade structure. Firstly, two extended disturbance observers (EDOs) are constructed to estimate the matched disturbances and the unmatched disturbance of the system and introduce them into the receding horizon optimization. Secondly, a novel dynamic horizon tuning mechanism is researched in this paper to improve control performance of the traditional generalized predictive control (GPC) which deviates from the optimal control under complex working conditions. Simulations show that the proposed GDPC is clearly superior to the cascade PI control and the GPC in terms of dynamic performance and disturbance rejection accuracy under changing working conditions.**

***Index Terms*—generalized predictive control, unmatched disturbance, dynamic horizon.**

I. Introduction

Permanent magnet synchronous motor (PMSM) has attracted broad attention due to its advantages of high energy density, high efficiency, and compact structure, which makes it widely used in high-precision applications such as robots, aerospace, and servo systems [1]. However, as the PMSM drive system is characterized by multivariable, multi-source disturbances, strong coupling, and non-linearity [2], the requirements for designing a simple, high-precision speed controller with fast dynamic response and excellent disturbance rejection ability are highly desirable [3].

Field-oriented control (FOC), as a traditional control framework, was proposed in 1969 [4], which controls the stator current to control torque directly, and it has a favorable steady-state performance and is widely used [5]. The cascade PI control method based on the FOC framework is still a mainstream control strategy in industrial control because of its virtues of intuitive parameter adjustment, simple control, and small calculation. Nevertheless, this method has poor disturbance rejection ability, and with the continuous improvement of industrial demand, it has gradually failed to meet the control performance requirement for some applications [6].

Besides, the cascade control structure consists of an inner current loop and an outer speed loop, although this method reduces difficulty of controller design, it limits the bandwidth of the system [7]. In the non-cascade structure, the current loop is omitted, and it can effectively improve the system dynamic response, but the torque load will be introduced into the system as the unmatched disturbance [8]. Furthermore, the traditional disturbance rejection strategies treat the system disturbances as the lumped disturbance, i.e., matched disturbance, such as extended state observer (ESO), while simple in design and making the system robust to disturbances, cannot estimate and compensate for unmatched disturbance.

In order to make the system have a faster dynamic response and high disturbance rejection capability, many advanced control strategies have been studied and proposed over the years, such as sliding mode control [9], model predictive control (MPC) [10], adaptive control [11], disturbance rejection control [8], and nonsmooth control [12], etc. Among these methods, MPC can effectively improve the system dynamic response, and with the revolutionary development of the microprocessors, it is a very promising control strategy.

This work was supported in part by the National Natural Science Foundation of China under Grant 62173221, 62203292 and in part by the Jiangsu Province Industry-University-Research Collaboration Project under BY2021304. (*Corresponding author: Jianliang Mao.*)

978-1-6654-9302-4/22/$31.00 © 2022 IEEE

Authorized licensed use limited to: Shanghai Univ of Electric Power. Downloaded on December 26,2022 at 14:04:34 UTC from IEEE Xplore. Restrictions apply.

However, this method is sensitive to the changes in the system model parameters. In [13], [10], the MPC combined with integrator or disturbance observer is proposed to solve this problem. But these methods can only compensate for the matched disturbances of the system but not for the unmatched disturbance, making it difficult to effectively reject the disturbance. Moreover, the computational burden is also the major obstacle to the application of this method to the practical applications with limited computing capacity. A generalized predictive control method was proposed in [14]. Compared with the online optimized model predictive control strategies above, this off-line optimization method with fixed horizon effectively reduces the computational burden, but this probably leads to the deviations in speed regulation from optimal performance under different working conditions in some practical applications.

In this paper, a GDPC method is proposed for the PMSM speed regulation system combined with disturbance observation techniques. Firstly, the method introduces both the estimated matched and unmatched disturbances into the receding horizon optimization to improve the disturbance rejection capability of the system. Secondly, a dynamic horizon tuning mechanism is developed in the paper, which can dynamically adjust the horizon according to system working conditions to maintain the system optimal control performance as much as possible under different working conditions. Finally, to verify the effectiveness of the proposed method, simulations are conducted in comparison with the traditional GPC and the cascade PI control methods.

II. Problem Formulation

A. Mathematical Model

The mathematical model of a surface-mounted PMSM in the d-q coordinate system is clearly described as [15]:

$$\begin{cases} \dot{\omega} = \dfrac{1}{J}(n_p\psi_f i_q - B\omega - T_L) \\ \dot{i_d} = \dfrac{1}{L_s}(-R_s i_d + n_p\omega L_s i_q + u_d) \\ \dot{i_q} = \dfrac{1}{L_s}(-R_s i_q - n_p\omega L_s i_d - n_p\psi_f\omega + u_q) \end{cases} \tag{1}$$

where i_d, i_q, u_d and u_q are the stator currents and voltages of the d-axis and the q-axis, respectively; ω is the mechanical angular velocity; n_p is the number of pole pairs; ψ_f is the rotor flux linkage; T_L is the load torque; B is the viscous frictional coefficient; J is the rotor inertia; R_s is the stator resistance and L_s is the stator inductance.

In this paper, we mainly focus on the effect of q-axis current on the system dynamic performance, and the d-axis current is assumed to be ideal tracking, i.e., $i_d = 0$.

B. Control Objective and Pre-treatment

The control objective of this paper is to achieve set speed tracking by constructing a GDPC approach in the presence of matched and unmatched disturbances.

Inspired by [8], the coordinate transformation is introduced for the system (1) as follows:

$$x_1 = \omega_{ref} - \omega,\ x_2 = \frac{1}{J}(-n_p\psi_f i_q + B\omega_{ref})$$

where ω_{ref} is the speed reference. Subsequently, the equivalent system is achieved in the following form:

$$\begin{cases} \dot{x}_1 = x_2 + f_1(x_1) + d_1 \\ \dot{x}_2 = u + f_2(x_1, x_2) + d_2 \\ y = x_1 \end{cases} \tag{2}$$

where $u = -\frac{n_p\psi_f}{JL_s}u_q$ is the control input, y is the system output, $d_1 = \frac{T_L}{J}$ is considered as the unmatched disturbance, d_2 are the matched disturbances that includes unmodelled dynamics and measurement errors, and the system dynamics

$$f_1(x_1) = -a_1 x_1,\ f_2(x_1, x_2) = -b_1 x_1 - b_2 x_2 + C \tag{3}$$

where

$$a_1 = \frac{B}{J}, b_1 = \frac{{n_p}^2\psi_f^2}{JL_s}, b_2 = \frac{R_s}{L_s},$$
$$C = \frac{1}{JL_s}(R_s B + {n_p}^2{\psi_f}^2)\omega_{ref}.$$

Assumption 1: The disturbances $d_1^{(r)}$ and $d_2^{(r)}$, $r = 0, 1, 2$ are bounded and satisfy $\lim_{t\to\infty} \ddot{d}_1(t) = 0$ and $\lim_{t\to\infty} \dot{d}_2(t) = 0$.

III. Controller Design

In this section, series of disturbance observers are built for estimating the information of the internal matched and unmatched disturbances. The performance compensation loop is designed in subsequent, and the optimal control law with the rigorous closed-loop stability analysis is naturally constructed.

A. Design of the Disturbance Observer

Aiming to achieve the estimation information of d_1 and d_2, the EDOs are designed as follows:

$$d_1 : \begin{cases} \dot{z}_{11} = -\beta_{11}(z_{11} - x_1) + x_2 + f_1(x_1) + z_{12} \\ \dot{z}_{12} = -\beta_{12}(z_{11} - x_1) + z_{13} \\ \dot{z}_{13} = -\beta_{13}(z_{11} - x_1) \end{cases} \tag{4}$$

$$d_2 : \begin{cases} \dot{z}_{21} = -\beta_{21}(z_{21} - x_2) + f_2(x_1, x_2) + u + z_{22} \\ \dot{z}_{22} = -\beta_{22}(z_{21} - x_2) \end{cases} \tag{5}$$

where β_{1i}, i=1, 2, 3, β_{2j}, j=1, 2 are observer gains, z_{11}, z_{12}, z_{13}, z_{21}, z_{22} are corresponding estimation of $x_1, d_1, \dot{d}_1, x_2, d_2$.

Define the observer estimation errors $\varepsilon_{11} = z_{11} - x_1$, $\varepsilon_{12} = z_{12} - d_1$, $\varepsilon_{13} = z_{13} - \dot{d}_1$, $\varepsilon_{21} = z_{21} - x_2$ and $\varepsilon_{22} = z_{22} - d_2$. Combining the observer system (4), (5) with system (2), the estimation errors dynamics are obtained as:

$$\Phi_1 : \begin{cases} \dot{\varepsilon}_{11} = -\beta_{11}\varepsilon_{11} + \varepsilon_{12} \\ \dot{\varepsilon}_{12} = -\beta_{12}\varepsilon_{11} + \varepsilon_{13}, \\ \dot{\varepsilon}_{13} = -\beta_{13}\varepsilon_{11} - \ddot{d}_1 \end{cases} \quad \Phi_2 : \begin{cases} \dot{\varepsilon}_{21} = -\beta_{21}\varepsilon_{21} + \varepsilon_{22} \\ \dot{\varepsilon}_{22} = -\beta_{22}\varepsilon_{21} - \dot{d}_2 \end{cases} \tag{6}$$

where $\varepsilon_1 = [\varepsilon_{11}, \varepsilon_{12}, \varepsilon_{13}]^\top$, $\varepsilon_2 = [\varepsilon_{21}, \varepsilon_{22}]^\top$ are the estimation errors.

Authorized licensed use limited to: Shanghai Univ of Electric Power. Downloaded on December 26,2022 at 14:04:34 UTC from IEEE Xplore. Restrictions apply.

B. Composite GDPC Design

At the beginning, combining the disturbance estimation z_{12}, z_{13} and z_{22} with the system dynamics (2), the steady reference signal of the system can be expressed as:

$$\begin{cases} x_1^* = 0,\ x_2^* = -z_{12} \\ u^* = -z_{13} - f_2(x_1^*, x_2^*) - z_{22}. \end{cases} \tag{7}$$

Define $e_1 = x_1 - x_1^*$, $e_2 = x_2 - x_2^*$, $\upsilon = u - u^*$. Then combining (7) and the system dynamics (2), the error system dynamics can be described as :

$$\begin{cases} \dot{e}_1 = e_2 + f_1(e_1) - \varepsilon_{12} \\ \dot{e}_2 = \upsilon + f_2(e_1, e_2) - \varepsilon_{22} \end{cases} \tag{8}$$

where $f_1(e_1) = f_1(x_1) - f_1(x_1^*), f_2(e_1, e_2) = f_2(x_1, x_2) - f_2(x_1^*, x_2^*)$.

1) Receding-Horizon Optimization: For the purpose of simplifying the analysis of the subsequent receding horizon optimization process, only the controllable parts of the system are considered. The error system (8) can be further simplified into the following integral-chain form:

$$\dot{e} = Ae + B\upsilon \tag{9}$$

where $e = [e_1, e_2]^\top$, $A = \begin{bmatrix} 0 & 1 \\ 0 & 0 \end{bmatrix}$, $B = [0, 1]^\top$.

The control order is selected as 0 (the specific definition is available in [16]), the future system output $\hat{e}_1$, within a horizon τ can be predicted by the Taylor series expansion as follow:

$$\hat{e}_1(t+\tau) \doteq e_1 + \tau e_2 + \frac{\tau^2}{2!}\upsilon = \overline{\mathcal{W}} e + \frac{\tau^2}{2!}\upsilon \tag{10}$$

where $\overline{\mathcal{W}} = [1, \tau]$.

To optimally converge the motor speed to a given reference value, the performance index is defined as:

$$\hat{J}(t) = \frac{1}{2}\int_0^T \hat{e}_1(t+\tau)^2 d\tau \tag{11}$$

where $T > 0$ is the horizon.

Substituting (10) into (11), one can obtain that

$$\begin{aligned} \hat{J}(t) &= \frac{1}{2}\int_0^T \hat{e}_1(t+\tau)^2 d\tau \\ &= \frac{1}{2} e^\top \overline{\mathcal{T}}_1 e + e^\top \overline{\mathcal{T}}_2 \upsilon + \frac{1}{2}\overline{\mathcal{T}}_3 \upsilon^2 \end{aligned} \tag{12}$$

where $\overline{\mathcal{T}}_1 = \begin{bmatrix} T & \frac{T^2}{2} \\ \frac{T^2}{2} & \frac{T^3}{3} \end{bmatrix}$, $\overline{\mathcal{T}}_2 = [\frac{T^3}{6}, \frac{T^4}{8}]^\top$, $\overline{\mathcal{T}}_3 = \frac{T^5}{20}$.

Taking partial derivative of $\hat{J}$ with respect to υ, one can get

$$\frac{\partial \hat{J}}{\partial \upsilon} = \overline{\mathcal{T}}_2^\top e + \overline{\mathcal{T}}_3 \upsilon \tag{13}$$

and the optimal control law of the system can be accurately obtained by letting (13) be zero, and expressed as:

$$\upsilon = -\overline{\mathcal{T}}_3^{-1}\overline{\mathcal{T}}_2^\top e \triangleq -\frac{k_1^*}{T^2}e_1 - \frac{k_2^*}{T}e_2. \tag{14}$$

Remark 1: Following (12) to (14), one can further calculated $k_1^* = 3.3$, $k_2^* = 2.5$, making the horizon T as the only parameter to be determined.

2) Design of the Dynamic Horizon Mechanism: the traditional GPC design method can not guarantee that the system has the optimal control performance under each working condition. For handling this situation, the proposed GDPC method can automatically adjust the appropriate parameter T according to the current system working conditions to try best to maintain optimal performance. To this aim, with the symbol T_0 as initial value of T, to be built self-tuning mechanism is:

$$T = \frac{T_0}{L}, T_0 > 0,\ \dot{L} = \rho(\frac{e_1^2}{L} + \frac{e_2^2}{L^2}), L(0) = 1 \tag{15}$$

where ρ is the updating gain, and L is the bandwidth factor.

Specifically, the optimal controller with dynamic horizon is:

$$u = -\frac{k_1^*}{T^2}e_1 - \frac{k_2^*}{T}e_2 + u^*. \tag{16}$$

The control block diagram is presented in Fig. 1.

Remark 2: It can be clearly seen from (16) that the proposed controller has a small computational burden and few control parameters. As for the problem of current limitation in practical applications, it can be effectively avoided by adjusting relatively conservative control parameters or employing current constraint design methods, such as [17].

C. Stability Analysis of Closed Loop System

Theorem 1: For system (2), combined with the constructed observers (4), (5) and the optimal control law (16) with dynamic horizon tuning mechanism, the closed-loop system is globally asymptotically stable, and the horizon T is bounded.

Proof: For the convenience of subsequent analysis, here utilizing coordinate transformation $\xi_1 = \frac{e_1}{L}$, $\xi_2 = \frac{e_2}{L^2}$, $\varsigma = \frac{\upsilon}{L^3}$, on the basis of (9), the following expressions can be obtained:

$$\begin{cases} \dot{\xi}_1 = L\xi_2 - \dfrac{\dot{L}}{L}\xi_1 + \dfrac{f_1(e_1)}{L} - \dfrac{\varepsilon_{12}}{L} \\ \dot{\xi}_2 = L\varsigma - 2\dfrac{\dot{L}}{L}\xi_2 + \dfrac{f_2(e_1, e_2)}{L^2} - \dfrac{\varepsilon_{22}}{L^2}. \end{cases} \tag{17}$$

Combining (6) and (16) with (17), we can further obtain the closed-loop system as follows:

$$\begin{cases} \dot{\xi} = L(A - BK)\xi - (I + \theta)\dfrac{\dot{L}}{L}\xi + F + \dfrac{E_1}{L}\varepsilon_1 + \dfrac{E_2}{L^2}\varepsilon_2 \\ \dot{\varepsilon}_1 = \bar{A}_1\varepsilon_1 + D_1,\ \dot{\varepsilon}_2 = \bar{A}_2\varepsilon_2 + D_2 \end{cases} \tag{18}$$

where

$$\xi = [\xi_1, \xi_2]^\top, K = [\frac{k_1^*}{T_0^2}, \frac{k_2^*}{T_0}], E_1 = [E_2, 0_{2\times 1}], E_2 = -A,$$

$$\theta = \begin{bmatrix} 0_{2\times 1}, B \end{bmatrix}, \bar{A}_1 = \begin{bmatrix} -\beta_{11} & 1 & 0 \\ -\beta_{12} & 0 & 1 \\ -\beta_{13} & 0 & 0 \end{bmatrix}, \bar{A}_2 = \begin{bmatrix} -\beta_{21} & 1 \\ -\beta_{22} & 0 \end{bmatrix},$$

$$\varepsilon_1 = [\varepsilon_{11}, \varepsilon_{12}, \varepsilon_{13}]^\top, \varepsilon_2 = [\varepsilon_{21}, \varepsilon_{22}]^\top, D_1 = [0, 0, \ddot{d}_1]^\top,$$

$$D_2 = [0, \dot{d}_2]^\top, F = [\frac{f_1(e_1)}{L}, \frac{f_2(e_1, e_2)}{L^2}]^\top.$$

Authorized licensed use limited to: Shanghai Univ of Electric Power. Downloaded on December 26,2022 at 14:04:34 UTC from IEEE Xplore. Restrictions apply.

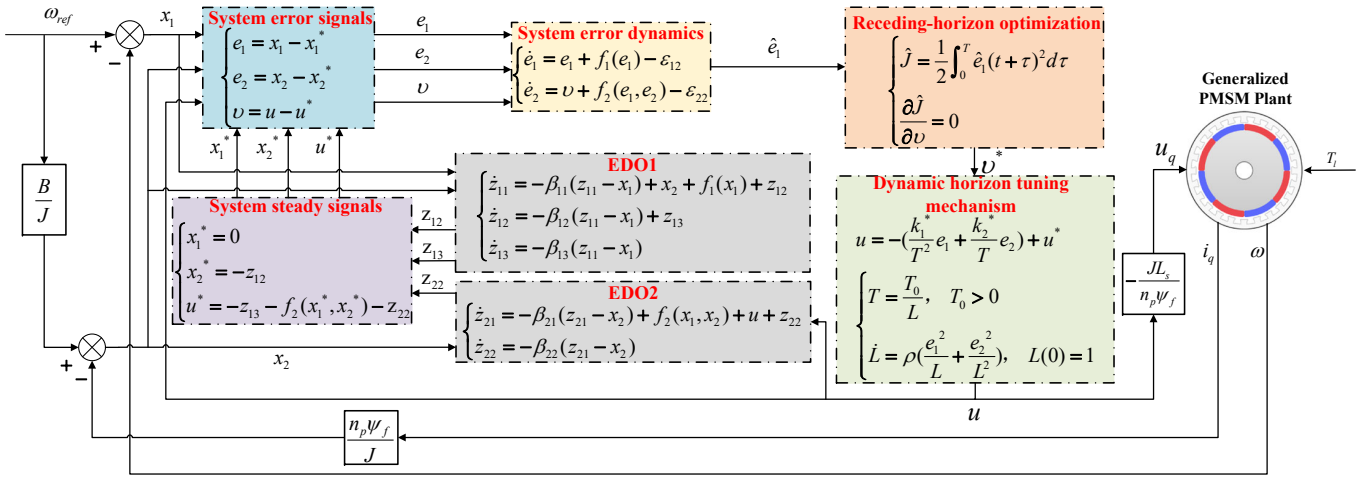

Fig. 1. Proposed controller block diagram.

The observer parameters are chosen to meet the matrices $\bar{A}_1$ and $\bar{A}_2$ are Hurwitz stable, i.e., there exist positive definite symmetric matrices P_1 and P_2 satisfying

$$\begin{cases} \bar{A}_1^\top P_1 + P_1 \bar{A}_1 = -I_{3\times 3} \\ \bar{A}_2^\top P_2 + P_2 \bar{A}_2 = -I_{2\times 2}. \end{cases} \tag{19}$$

After defining $\kappa_1 = \frac{k_1^*}{T_0^2}, \kappa_2 = \frac{k_2^*}{T_0}$, and clearly $\kappa_1 > 0, \kappa_2 > 0$, one can get that the matrix $(A - BK)$ is always Hurwitz stable, then we arrive at

$$(A - BK)^\top Q + Q(A - BK) = -I_{2\times 2} \tag{20}$$

where $Q = Q^\top > 0$. Furthermore, it can be calculated as

$$Q = \frac{1}{2}\begin{bmatrix} \frac{\kappa_1+\kappa_1^2+\kappa_2^2}{\kappa_1\kappa_2} & \frac{1}{\kappa_1} \\ \frac{1}{\kappa_1} & \frac{1+\kappa_1}{\kappa_1\kappa_2} \end{bmatrix}.$$

Choose a candidate Lyapunov function as following:

$$V(\xi, \varepsilon_1, \varepsilon_2) = \xi^\top Q \xi + \varepsilon_1^\top P_1 \varepsilon_1 + \varepsilon_2^\top P_2 \varepsilon_2. \tag{21}$$

For analysis convenience, define the matrix $H = Q(I_{2\times 2} + \theta) + (I_{2\times 2} + \theta)Q$. Then taking the time derivative of $V(\xi, \varepsilon_1, \varepsilon_2)$ along the closed-loop system dynamics (18) gives

$$\begin{aligned} \dot{V} &\le -L\|\xi\|^2 - \frac{\dot{L}}{L}\xi^\top H \xi - \|\varepsilon_1\|^2 - \|\varepsilon_2\|^2 + 2F^\top Q\xi \\ &\quad + 2\xi^\top Q E_1 \varepsilon_1 + 2\xi^\top Q E_2 \varepsilon_2 + 2D_1^\top P_1 \varepsilon_1 + 2D_2^\top P_2 \varepsilon_2 \\ &\le -L\|\xi\|^2 - \|\varepsilon_1\|^2 - \|\varepsilon_2\|^2 + 2\lambda_{\max}(Q)\|\xi\|\|F\| \\ &\quad + 2\lambda_{\max}(P_1)\|D_1\|\|\varepsilon_1\| + 2\lambda_{\max}(P_2)\|D_2\|\|\varepsilon_2\| \\ &\quad + \lambda_{\max}(Q)\big(2\|\xi\|^2 + \|\varepsilon_1\|^2 + \|\varepsilon_2\|^2\big). \end{aligned} \tag{22}$$

Combining (3) and (8), one gets $F = -[\frac{a_1 e_1}{L}, \frac{b_1 e_1 + b_2 e_2}{L^2}]^\top$, then $\|F\| \le 2\mu\|\xi\|$ holds with $\mu = \max\{a_1, b_1, b_2\}$, and the following relationship can be further obtained:

$$\dot{V} \le -(L - \ell_1)\|\xi\|^2 - \|\varepsilon_1\|^2 - \|\varepsilon_2\|^2 + E \tag{23}$$

where $\ell_1 = 2\lambda_{\max}(Q)(1 + 2\mu)$, $E = 2\lambda_{\max}(P_1)\|D_1\|\|\varepsilon_1\| + 2\lambda_{\max}(P_2)\|D_2\|\|\varepsilon_2\| + \lambda_{\max}(Q)(\|\varepsilon_1\|^2 + \|\varepsilon_2\|^2)$, and $\lambda_{\max}(\cdot)$, $\lambda_{\min}(\cdot)$ represent the maximum and minimum eigenvalues of the matrix $(\cdot)$, respectively.

With Assumption 1 in mind, there exists a bounded constant Γ such that $\sup\{|\varepsilon_{1i}|, |\varepsilon_{2j}|\} \le \Gamma, i = 1, 2, 3, \ j = 1, 2,$ $\forall t \in [0, +\infty)$. Therefore, it is natural to get that there exists a bounded constant $\mathcal{E}$ related to Γ such that for any $L > \ell_1 + 1$, the following inequality holds:

$$\dot{V} \le -\|\xi\|^2 - \|\varepsilon_1\|^2 - \|\varepsilon_2\|^2 + \mathcal{E} \le -\gamma_0 V + \mathcal{E} \tag{24}$$

where $\gamma_0 > 0$, denoted by

$$\gamma_0 = \frac{1}{\max\{\lambda_{\max}(Q), \lambda_{\max}(P_1), \lambda_{\max}(P_2)\}}.$$

At this time, the solution of (24) can be calculated as

$$V(t) \le e^{-\gamma_0(t-t_0)}V(t_0) + \int_{t_0}^{t} e^{-\gamma_0(t-\tau)}\mathcal{E}d\tau. \tag{25}$$

From (25), we can conclude that $\lim_{t\to\infty} V(t) = 0$, i.e., the closed-loop system is globally asymptotically stable.

We can further see from (25) that L changes continuously with the state of the system, so there is a problem of whether L will diverge. Next, we will prove the boundedness of L, i.e., to prove that T is bounded. To begin with, suppose that L will diverge to infinity in finite time instant t_1, i.e., $\lim_{t\to t_1} L(t) = \infty$. There exists a finite time $t^* \in [0, t_1)$ satisfying $L(t^*) > \ell_1 + 1$, i.e., (24) holds $\forall t \in [t^*, t_1)$. Furthermore, the following relationship can be obtained:

$$\begin{aligned} +\infty &= \int_{t^*}^{t_1} \dot{L}(t)dt = \rho\int_{t^*}^{t_1}(\frac{e_1^2}{L} + \frac{e_2^2}{L^2})dt \le \rho\int_{t^*}^{t_1}\|\xi\|^2 dt \\ &\le \int_{t^*}^{t_1} \mathcal{E} - \rho\dot{V}(t)dt = \rho(V(t^*) - V(t_1)) + \mathcal{E}(t_1 - t^*) \\ &= \textbf{constant}. \end{aligned}$$

Hence, it contradicts the assumption above. Furthermore, we can conclude that L has an upper bound in $t \in [0, +\infty)$, i.e., T has a lower bound in $t \in [0, +\infty)$. ■

Authorized licensed use limited to: Shanghai Univ of Electric Power. Downloaded on December 26,2022 at 14:04:34 UTC from IEEE Xplore. Restrictions apply.

IV. Simulation Validations

In this section, to verify the effectiveness of the proposed control method, a simulation comparison is realized by using MATLAB/Simulink tool. Where the cascade PI control and the conventional GPC approaches combined with ESO are taken as the comparison group, and physical parameters of the PMSM are given in Table I.

TABLE I
PARAMETERS OF THE PMSM SYSTEM

Symbol	Quantity	Nominal values
n_p	Poles	4
R_s	Stator resistance	0.36Ω
L_s	Stator inductance	2.0×10^{-4}mH
ψ_f	Flux linkage	0.0064Wb
J	Rotor inertia	7.066×10^{-6} kg·m^2
B	Viscous damping	2.637×10^{-6}N·m·s/rad
$\omega_{\max}$	Max speed	6000rpm
I_N	Rated current	7.1A
V_{dc}	Line voltage	24V

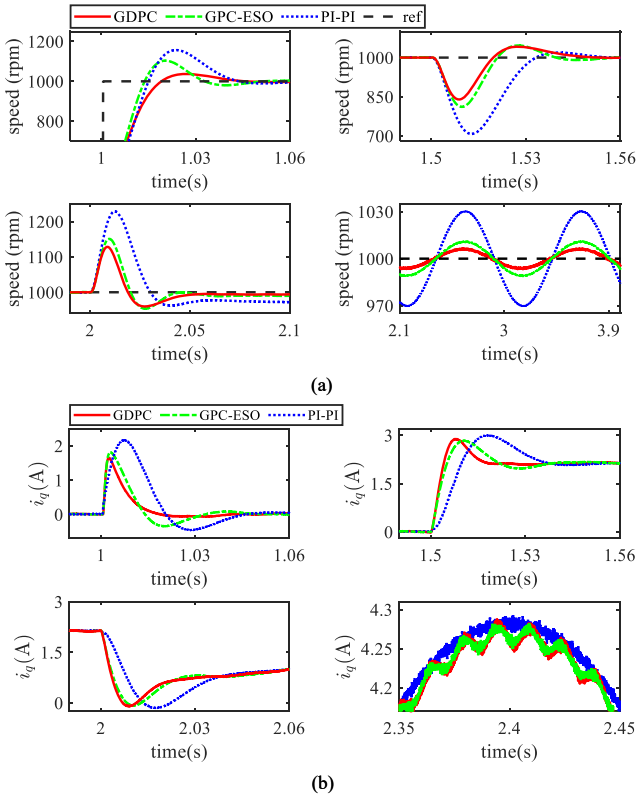

Fig. 2. System responses: (a) motor speed, (b) q-axis current i_q (simulations).

Fig. 2 presents the simulation results of the cascade PI controller, the GPC with ESO, and the proposed GDPC. The test condition is that the speed reference step from 500 to 1000rpm is applied at t = 1s, and at t = 2s the 30% nominal load torque 0.0817 N·m is applied on the motor, then the sinusoidal load torque $0.0817\sin(2\pi t + 1.7\pi)$ N·m is applied at t = 4s. The first channel shows the reference and actual

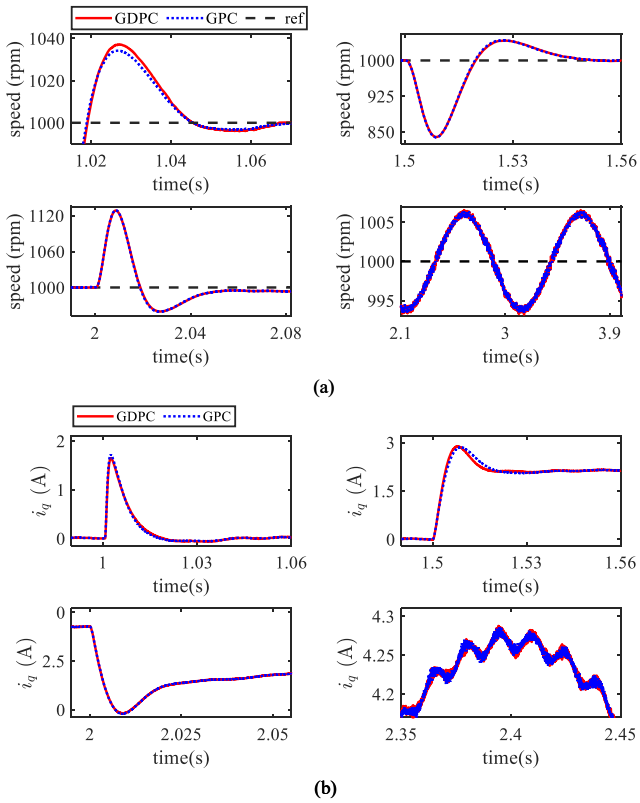

Fig. 3. System responses in working condition 1: (a) motor speed, (b) q-axis current i_q (simulations).

speed curves, and the second channel shows the q-axis current curves. It is seen from Fig. 2 the proposed controller GDPC has a smaller overshoot in transient stage, followed by the GPC. Step load is applied at t = 2s, the GDPC has the smallest speed drop compared with other controllers. After t = 4s sinusoidal disturbance is applied, it can be clearly seen that the speed fluctuation of the proposed GDPC is the smallest, and the GPC is second only to GDPC. We can conclude from the simulations above that the proposed GDPC has the best dynamic performance and disturbance rejection ability.

In addition, to verify the effectiveness of the proposed dynamic horizon mechanism, a comparison is made between the controller that with and without this mechanism under different working conditions, and the other structures of the controller are identical. Working condition 1 is the same as the test condition in Fig. 2. Working condition 2 is based on working condition 1, and the reference speed step is set as from 500 to 2000rpm at t=1s. For a more visible contrast, the control parameters are adjusted so that the control performance of the two controllers is nearly the same under working condition 1, and then switch to the working condition 2 to compare the control performance. Fig. 3 and Fig. 4 present the simulation results, it is seen from Fig. 3 that the control performance of the two controllers is roughly the same in working condition 1, and from Fig. 4 can be seen that the controller with a dynamic horizon mechanism has a

Authorized licensed use limited to: Shanghai Univ of Electric Power. Downloaded on December 26,2022 at 14:04:34 UTC from IEEE Xplore. Restrictions apply.

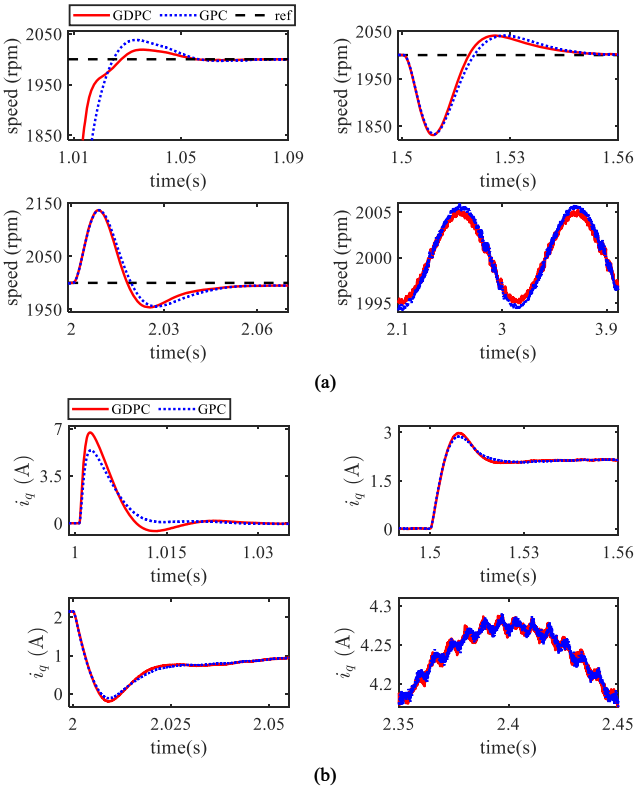

Fig. 4. System responses in working condition 2: (a) motor speed, (b) q-axis current i_q (simulations).

faster response speed and smaller overshoot in the working condition 2, and the speed fluctuation under the sinusoidal disturbance becomes smaller, i.e., the disturbance rejection ability is enhanced.

According to the analysis of simulation results above, we can conclude that the proposed GDPC improves the disturbance rejection ability and dynamic response speed of the PMSM drive system, and can maintain satisfactory control performance under different working conditions.

V. CONCLUSION

This article proposed a GDPC method based on EDOs for the PMSM speed regulation system in which the non-cascade structure is adopted, and a dynamic horizon mechanism is designed. In order to verify the effectiveness of the proposed method, simulation analysis and comparison are made between the proposed method, the GPC and the cascade PI control. The simulation results confirmed that the proposed method achieves fast dynamic response, satisfiable disturbance rejection ability, and enhances the system control performance under changed working conditions.

REFERENCES

[1] P. Kakosimos and H. Abu-Rub, "Predictive speed control with short prediction horizon for permanent magnet synchronous motor drives," *IEEE Transactions on Power Electronics*, vol. 33, no. 3, pp. 2740–2750, 2018.

[2] Y. Wang, Y. Feng, X. Zhang, and J. Liang, "A new reaching law for antidisturbance sliding-mode control of pmsm speed regulation system," *IEEE Transactions on Power Electronics*, vol. 35, no. 4, pp. 4117–4126, 2020.

[3] Y. Shi, J. Chai, X. Sun, and S. Mu, "Detailed description and analysis of the cross-coupling magnetic saturation on permanent magnet synchronous motor," *The Journal of Engineering*, vol. 2018, no. 17, pp. 1855–1859, 2018.

[4] Y. Yan, S. Wang, C. Xia, W. H, and T. Shi, "Hybrid control set-model predictive control for field-oriented control of vsi-pmsm," *IETE Transactions on Energy Conversion*, vol. 31, no. 4, pp. 1622–1633, 2016.

[5] Y. Zhang, J. Jin, and L. Huang, "Model-free predictive current control of pmsm drives based on extended state observer using ultralocal model," *IEEE Transactions on Industrial Electronics*, vol. 68, no. 2, pp. 993–1003, 2020.

[6] W. Xu, A. K. Junejo, Y. Liu, and M. R. Islam, "Improved continuous fast terminal sliding mode control with extended state observer for speed regulation of pmsm drive system," *IEEE Transactions on Vehicular Technology*, vol. 68, no. 11, pp. 10 465–10 476, 2019.

[7] A. M. Diab, S. Bozhko, F. Guo, M. Rashed, G. Buticchi, Z. Xu, S. S. Yeoh, C. Gerada, and M. Galea, "Fast and simple tuning rules of synchronous reference frame proportional-integral current controller," *IEEE Access*, vol. 9, pp. 22 156–22 170, 2021.

[8] C. Dai, T. Guo, J. Yang, and S. Li, "A disturbance observer-based current-constrained controller for speed regulation of pmsm systems subject to unmatched disturbances," *IEEE Transactions on Industrial Electronics*, vol. 68, no. 1, pp. 767–775, 2020.

[9] X. Zhang, L. Sun, K. Zhao, and L. Sun, "Nonlinear speed control for pmsm system using sliding-mode control and disturbance compensation techniques," *IEEE Transactions on Power Electronics*, vol. 28, no. 3, pp. 1358–1365, 2012.

[10] L. Yan, M. Dou, and Z. Hua, "Disturbance compensation-based model predictive flux control of spmsm with optimal duty cycle," *IEEE Journal of Emerging and Selected Topics in Power Electronics*, vol. 7, no. 3, pp. 1872–1882, 2019.

[11] S. Li and Z. Liu, "Adaptive speed control for permanent-magnet synchronous motor system with variations of load inertia," *IEEE Transactions on Industrial Electronics*, vol. 56, no. 8, pp. 3050–3059, 2009.

[12] X. Dong, C. Zhang, T. Yang, and J. Yang, "Nonsmooth dynamic tracking control for nonlinear systems with mismatched disturbances: Algorithm and practice," *IEEE Transactions on Industrial Electronics*, 2022, doi: 10.1109/TIE.2022.3181367.

[13] A. A. Ahmed, B. K. Koh, and Y. I. Lee, "A comparison of finite control set and continuous control set model predictive control schemes for speed control of induction motors," *IEEE Transactions on Industrial Informatics*, vol. 14, no. 4, pp. 1334–1346, 2017.

[14] M. Shao, Y. Deng, H. Li, J. Liu, and Q. Fei, "Robust speed control for permanent magnet synchronous motors using a generalized predictive controller with a high-order terminal sliding-mode observer," *IEEE Access*, vol. 7, pp. 121 540–121 551, 2019.

[15] T. Guo, Z. Sun, X. Wang, S. Li, and K. Zhang, "A simple current-constrained controller for permanent magnet synchronous motor," *IEEE Transactions on Industrial Informatics*, vol. 15, no. 3, pp. 1486–1495, 2019.

[16] W. H. Chen, D. J. Ballance, and P. J. Gawthrop, "Optimal control of nonlinear systems: a predictive control approach," *Automatica*, vol. 39, no. 4, pp. 633–641, 2003.

[17] J. Mao, H. Li, L. Yang, H. Zhang, L. Liu, X. Wang, and J. Tao, "Non-cascaded model-free predictive speed control of smpmsm drive system," *IEEE Transactions on Energy Conversion*, vol. 37, no. 1, pp. 153–162, 2022.

Authorized licensed use limited to: Shanghai Univ of Electric Power. Downloaded on December 26,2022 at 14:04:34 UTC from IEEE Xplore. Restrictions apply.